https://doi.org/10.5194/acp-2020-617
Preprint. Discussion started: 11 August 2020

Atmospheric Chemistry and Physics Discussions

PM2.5 surface concentrations in southern West African urban areas based on sun photometer and satellite observations

Jean-François Léon[1], Aristide Barthélémy Akpo[2], Mouhamadou Bedou[3], Julien Djossou[2], Marleine Bodjrenou[2], Véronique Yoboué[3], and Cathy Liousse[1]

[1]Laboratoire d'Aérologie, Université Paul Sabatier, CNRS, Toulouse, France
[2]Laboratoire de Physique du Rayonnement, Université d'Abomey Calavi, BP 526, Cotonou, Bénin
[3]Laboratoire de Physique de l'atmosphère, Université Félix-Houphouët-Boigny, Abidjan, Côte d'Ivoire

Correspondence: Jean-François Léon (jean-francois.leon@aero.obs-mip.fr)

Abstract. Southern West Africa (sWA) is influenced by large amounts of aerosol particles of both anthropogenic and natural origins. Anthropogenic aerosol emissions are expected to increase in the future due to the economical growth of African megacities. In this paper, we investigate the aerosol optical depth (AOD) in the coastal area of the Gulf of Guinea using sun photometer and MODIS satellite observations. We use a lightweight handheld sun photometer measuring the solar irradiance at 465, 540 and 619 nm operated manually every day from December 2014 to April 2017 at 5 different locations in Côte d'Ivoire and Bénin. Handheld sun photometer observations are complemented by available AERONET sun photometer observations and MODIS level 3 time series between 2003 and 2018. MODIS daily level 3 AOD agrees well with sun photometer observations in Abdidjan and Cotonou (correlation coefficient R=0.89 and RMSE=0.19). A classification based on the Angstrom Exponent is used to separate the influence of coarse mineral dust and urban-like aerosols. The AOD seasonal pattern is similar for all the sites and is clearly influenced by the mineral dust advection from December to May. AODs are analyzed in coincidence with surface PM2.5 concentrations to infer trends in the particulate pollution levels over conurbation of Abidjan (Côte d'Ivoire) and Cotonou (Bénin). PM2.5 to AOD conversion factors are evaluated as a function of the season and the aerosol type identified in the AE classification. Highest PM2.5 concentrations (up to 300 $\mu g/m^3$) are associated to the advection of mineral dust in the heart of the dry season (December-February). From December to March the median concentration above Abidjan and Cotonou is around 40 $\mu g/m^3$, while it is around 20 $\mu g/m^3$ during the rest of the year. Considering only the days during which the AOD belongs to the urban-like aerosol category, we observe a significant trend S=0.32 $\mu g/m^3/year$ in the PM2.5 concentrations over the period 2003-2017. This trend leads to an increase of 5 $\pm$ 3 $\mu g/m^3$ over 15 years and is coherent with the expected increase in combustion aerosol emissions in sWA.

https://doi.org/10.5194/acp-2020-617
Preprint. Discussion started: 11 August 2020

Atmospheric Chemistry and Physics Discussions

1 Introduction

The increasing trend in the anthropogenic emissions in Africa (Liousse et al., 2014) gives rise to the question of the impact of human activities on air quality, the monsoon system and the regional climate. The Gulf of Guinea and adjacent countries, hereinafter called southern West Africa (sWA), is influenced by large amounts of aerosol particles of both anthropogenic and natural origins advected from the African continent. The season cycle in sWA is driven by the monsoon system (Knippertz et al., 2015) with the alternation of a major winter (November to March) dry season and a summer (June-July) rainy season. The Inter Tropical Front (Lélé and Lamb, 2010) is at its southernmost position during the winter dry season enabling the northeasterly Harmattan wind to carry a dust-laden dry air southward (Adetunji et al., 1979). The major conurbations of sWA are then downwind the mineral dust emission of the Bodélé depression, the predominant dust emission source of West Africa (Todd et al., 2007; Washington, 2005; Koren et al., 2006; Schepanski et al., 2009). Carbonaceous aerosols that are emitted by open biomass burning (Liousse et al., 2010) are also advected southward to the main coastal cities of sWA during the dry period. The summer wet season corresponds to the continental intrusion of the southwesterly monsoon winds carrying moist air and precipitation. During this period, biomass burning emissions in central Africa can be advected to sWA by easterly wind and thus can impact the local air quality of coastal conurbations (Menut et al., 2018).

sWA is a hot spot of atmospheric aerosol concentrations as revealed by satellite-derived aerosol optical depth (Kaufman et al., 2002). The aerosol optical depth (AOD) is a key parameter for assessing the aerosol direct radiative impact (Boucher et al., 2013), which is of primary importance for the regional climate and the monsoon system (Janicot, 1992). AOD is the primary aerosol optical parameter derived from satellite remote sensing (Kaufman et al., 1997). AOD is related to the reduction in the atmospheric transmission due to aerosol particles in suspension in the atmosphere. AOD can be measured directly from the ground by using a sun photometer (Volz, 1959; Prospero et al., 1979; Tanré et al., 1988; Nakajima et al., 1996). The Aerosol Robotic Network (Holben et al., 1998, 2001) is one of the most important federated network of ground-based automatic sun photometers providing continuous AOD measurements in many places of the world. Western Africa benefits from a good geographical coverage of AERONET sun photometers in the Sahel transect. The stations are located in remote places dedicated to the monitoring of Saharan dust or biomass burning aerosols optical properties and atmospheric transport (Tanré et al., 1988; Redelsperger et al., 2006; Mallet et al., 2008; Léon et al., 2009). However sun photometer observations in the large conurbations surrounding the gulf of Guinea remain scarce. AOD observations in the coastal part of sWA will thus provide additional ground-truths for satellite validation.

Long-term satellite-derived AOD can also make up for the lack of in situ particulate matter (PM) surface observations. As air quality in sWA conurbations is still poorly covered by operational observational networks, satellite-derived PM may have a significant added-value for air quality monitoring. There is an abundant literature on linking columnar satellite AOD to PM (Kacenelenbogen et al., 2006; Hoff and Christopher, 2009; Ma et al., 2015; van Donkelaar et al., 2016). The relationship between instantaneous AOD and PM measurements is not straightforward and several regression models have been tested, either linear (Kacenelenbogen et al., 2006), multi-linear (Gupta and Christopher, 2009) or non-linear (Gupta and Christopher, 2009; Yahi et al., 2013; Kamarul Zaman et al., 2017). The conversion model from AOD to PM depends on the aerosol physical

https://doi.org/10.5194/acp-2020-617
Preprint. Discussion started: 11 August 2020


Atmospheric Chemistry and Physics Discussions

properties (aerosol type), hygroscopicity and the atmospheric dynamics including boundary layer mixing. Additional local analysis of the PM-to-AOD relationship based on in situ observations will strengthen the systematic retrieval of PM for satellite remote sensing.

In a companion paper (Djossou et al., 2018), the AOD measurements obtained downtown major cities of Abidjan (Côte d'Ivoire) and Cotonou (Bénin) were presented along with the surface observations of the PM2.5 mass concentration and carbonaceous aerosol composition. A tentative analysis of the relationship between AOD and PM2.5 was made and show the potential of AOD to infer PM2.5 concentration in both conurbations. In this paper, we report additional AOD measurements over sWA using lightweight handheld and automatic sun photometer with the purpose of validating the MODIS-derived AOD at the regional scale and investigating further the use of AOD for local pollution assessment. Section 2 presents the data sets and the methods. Section 3 presents the sun photometer time series the validation to the satellite AODs. The relationship between AOD and PM2.5 is investigated in section 4. The last section presents the interannual trends in PM2.5 derived from the MODIS observations.

2 Data and Method

All the observations were acquired in a geographical box ranging from approximately 4° N to 9° N and 6° W to 5° E (Figure 1) The domain is bounded at its southern part by the gulf of Guinea and at its northern part by the sudanian savanna and desertic areas of Sahel and encompasses guinea savanna and forest ecosystems. Major conurbations are located on the shore of the gulf of Guinea: Abidjan (Côte d'Ivoire), Accra (Ghana), Lomé (Togo), Cotonou (Bénin) and Lagos (Nigeria). We have collected observations at 3 coastal locations, namely Abidjan, Cotonou and Koforidua, and 4 inland locations, namely Savè, Lamto, Ilorin and Comoé, (see Table 1 for geographical coordinates). The sites labelled Abidjan and Cotonou are respectively located downtown the city of Abidjan (≈ 4.4 million inh.) and the conurbation of Cotonou (≈ 1,7 million inh. including satellite cities). Savè site is located in the medium-sized city of Savè (≈ 90,000 inh.). Lamto is a rural remote site located 200 km north of Abidjan. Comoé site is located near the village of Nassian at the southern edge of La Comoé natural reserve. Ilorin site is located at the Department of Physics on the campus of the University of Ilorin (≈ 800,000 inh.) in Nigeria. Koforidua site is located at the main campus of All Nations University College about 5 km from Koforidua City (≈ 120,000 inh.), 50 km north of Accra, Ghana.

2.1 Sun photometers

Table 1 summarizes the location, type of instrument and observation periods. We have used different types of sun photometers, automatic and handhelds. The automatic CIMEL sun photometer is the reference instrument used in the AERONET network (Holben et al., 1998) for measuring the AOD and retrieve columnar aerosol optical properties and size distribution. We have used the level 2 quality assured data processed with the version 3 of the aerosol optical depth algorithm (Giles et al., 2019). We used the data for Ghana (station named Koforidua_ANUC located at 6° 6' N, 0° 6' W), Nigeria (station named Ilorin located

https://doi.org/10.5194/acp-2020-617
Preprint. Discussion started: 11 August 2020

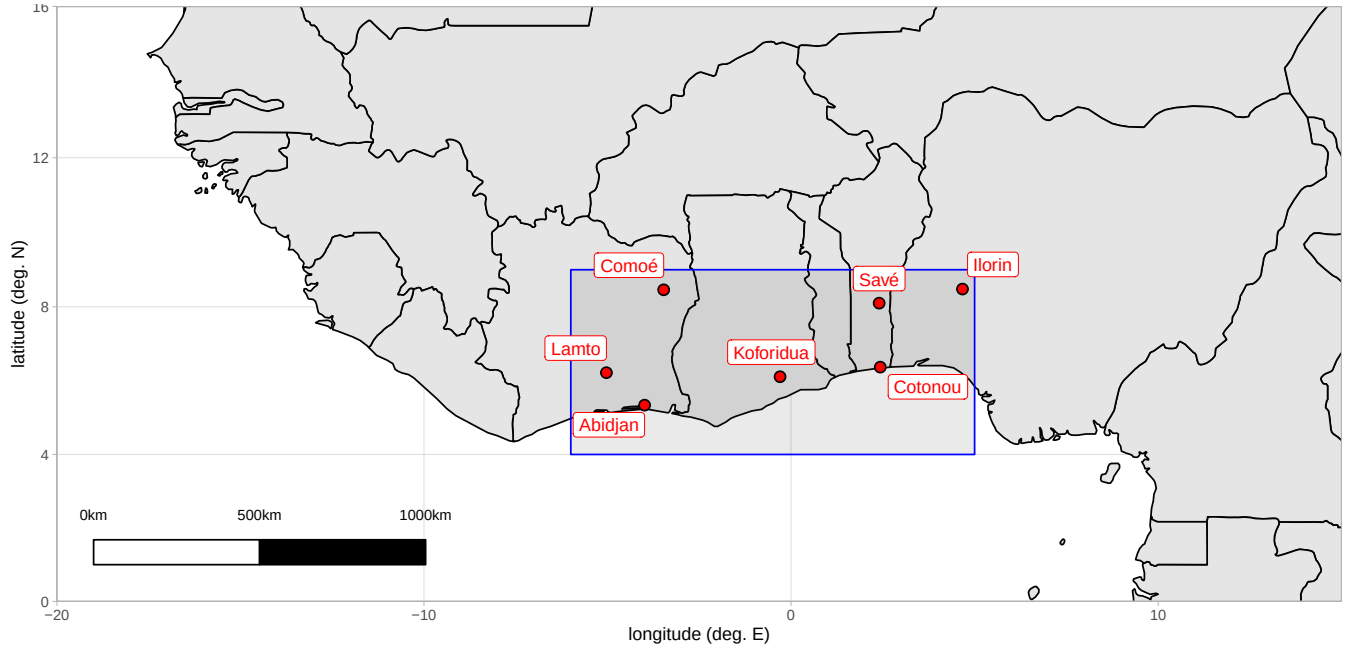

Figure 1. Geographical locations of the sun photometer sites in south Western Africa.

at 8° 29' N, 4° 40' E) and Côte d'Ivoire (station named Lamto located at 6° 13' N, 5° 2' W). The geophysical station of Lamto was early equipped in 1997-1998 then the automatic sun photometer was restored back in 2017.

Handheld sun photometer is a well-known scientific instrumentation for measuring atmospheric transmission (Porter et al., 2001; Volz, 1959, 1974). The first type of handheld photometer we used is the one manufactured by CIMEL, hereinafter called HHC. HHC was operated during 2 years between April 2006 and March 2008 at Lamto geophysical station. The operating wavelengths are 440, 670 and 870 nm. The second handheld sun photometer is a new lightweight instrument manufactured by TENUM (http://www.calitoo.fr) and named CALITOO (Djossou et al., 2018). CALITOO operating wavelengths for the CALITOO are 465 nm, 540 nm and 619 nm. The sun photometer measures the Sun irradiance at the 3 wavelengths. The atmospheric optical depth is then retrieved following the Beer-Lambert law knowing the calibration constant for each instrument and the relative air mass. The AOD is then retrieved after subtracting the Rayleigh and trace gases optical depth.

For the HHC, observations were acquired twice a day at around 9:00 and 15:00 UTC. For the CALITOO sun photometer, the observations were acquired at around 13:00 LT. The operators were asked to make measurements only when the sun was not obscured by clouds and have proceed with a sequence of 5 measurements within about 15 minutes. The presence of subvisible cirrus or broken clouds within the field of view induces spurious variation in the atmospheric transmission (Smirnov et al., 2000) that can be easily detected by looking at the standard deviation of the 15-minute series of AOD measurements. An arbitrary threshold of 0.2 on the standard deviation has been selected to remove the cloud-contaminated observations.

https://doi.org/10.5194/acp-2020-617
Preprint. Discussion started: 11 August 2020


Atmospheric Chemistry and Physics Discussions

The diurnal variability range is expected to be less than 10% for our site conditions (Smirnov, 2002). The sun photometer observations are reported as daily averages.

The total uncertainty in AOD for the AERONET instruments is ± 0.01 for $\lambda > 440nm$ and ± 0.02 for shorter wavelengths (Holben et al., 1998). CALITOO sun photometers were calibrated prior to the site deployment using the Langley-plot method (Soufflet et al., 1992; Schmid and Wehrli, 1995) at the Izaña high-altitude observatory (Basart et al., 2009). A direct comparison with a AERONET instrument indicates that the total uncertainty in AOD for CALITOO is ± 0.02 for all the wavelengths. The post-field calibration was done using a reference AERONET instrument and indicates a change of about 1% per year in the calibration.

AOD measurements are all reported at 550 nm because this wavelength is a reference for visibility calculation (Boers et al., 2015) and satellite mission (e.g. Remer et al., 2008). The Angström exponent (AE) (Angström, 1961) is computed between wavelengths 465 and 619 nm for the CALITOO and 440 and 670 nm for the HHC, and between 440 and 675 nm for the AERONET.

2.2 Satellite data

The Moderate Resolution Imaging Spectroradiometer (MODIS) aerosol products (Remer et al., 2005, 2008) have been widely used by the scientific community for assessing the impact of aerosols on global climate (Boucher et al., 2013) or air quality (van Donkelaar et al., 2016). The MODIS AOD is also used in operational data assimilation for weather forecast (Benedetti et al., 2009; Lynch et al., 2016). We have used the daily MODIS AOD at 550 nm from AQUA satellite (namely MYD08_D3) from 2003 to 2018. The spatial resolution of the MODIS product is $1^\circ \times 1^\circ$. We use the product named AOD_550_Dark_Target _Deep_Blue_Combined_Mean and Deep_Blue_Angstrom_Exponent_Land_Mean from the version 6 (Levy et al., 2013) of the MODIS processing algorithm, which is a combination of the "Dark target" (Levy et al., 2010) and "Deep blue" (Sayer et al., 2013) methods. For the purpose of satellite validation, the satellite AOD and AE of the nearest cell to the photometer location are extracted. We have adopted the evaluation metrics proposed by Sayer et al. (2014) including the linear correlation coefficient, the median bias, the root mean square error, the mean absolute percentage error, and the fraction of data falling within the MODIS expected error (EE) given by $EE = \pm 0.05 + 0.15 \times AOD$.

2.3 Surface concentration observations

From February 2015 to March 2017, Abidjan and Cotonou were equipped with PM2.5 monitoring stations (Djossou et al., 2018). Particles were collected on 47 mm diameter filters (quartz and PTFE filter types) at a flow rate of 5 L/min. Samplers were equipped with a PM2.5 mini Partisol impactor. PTFE filter were weighted before and after the sampling with a microbalance Sartorius MC21S. PM2.5 mass concentrations are estimated from the mass load on the filters and the total volume of air sampled measured by a GALLUS-type G4 gas meter. Exposure duration of the filter is one week. We have used the PM2.5 weekly observations collected at the urban site named “traffic” in Cotonou and the mean value at the two urban sites named “traffic” and “landfill” in Abidjan. In section 4, the AOD and AE are weekly averaged for the sake of comparison between PM2.5 and sun photometer observations.

https://doi.org/10.5194/acp-2020-617
Preprint. Discussion started: 11 August 2020

Atmospheric Chemistry and Physics Discussions

3 Sun photometer results

3.1 Daily statistics

A total of 2323 handheld sun photometer observations (including data collected during the 2006 campaign) have been acquired. Starting and ending dates are reported in table 1 along with the number of observations, median and interquartile range (IRQ) of AOD and AE distributions. We select the AERONET data until the end of the CALITOO observation period, i.e October 2017 for a total number of 1248 daily observations. There is an excellent time coverage for the stations of Lamto and Cotonou by the CALITOO observations. Observations were performed for 66% of the time in Cotonou, and 68% in Lamto. As a comparison, this rate is 68% for the automatic sun photometer in Koforidua, indicating that handheld measurements can be as representative as the automatic ones. This rate drops to 24% in Abidjan, 39% in Savè due to operating issues leading to gaps in the time series.

The overall range of AOD is (0.07, 3.8). The highest AOD acquired by the CALITOO instrument is 3.5 in Cotonou in March 2015 and the highest AOD recorded by the AERONET sun photometer is 3.7 in Ilorin in Dec. 2016. The median AOD ranges between a minimum of 0.47 at Lamto and maximum of 0.66 at Comoé. Considering all the daily measurements for all the sites, the median AOD is 0.52, IQR=(0.33, 0.82). AOD observations at Cotonou and Abidjan are rather similar, with a median AOD=0.55 (0.38, 075) and 0.58 (0.35, 0.86), respectively. The observations with the automatic sun photometer in Koforidua shows AOD in the same range as the 2 aforementioned stations, with a median AOD=0.49 (0.33, 0.84). The observations performed at Lamto with the 3 kinds of sun photometers show similar AOD: 0.47 (0.3, 0.72), 0.55 (0.35, 0.80) and 0.56 (0.38, 0.85) for CALITOO, HHC and AERONET respectively.

The median AE is between a minimum of 0.33 (0.13, 0.55) at Comé and a maximum of 0.78 (0.56, 1.09) at Koforidua. Observations performed with CALITOO at Lamto shows a lower range of AE values than the ones performed with the HHC and AERONET. The bias toward lower AE is about -0.1. AEs in Cotonou AE=0.58 (0.32, 0.89) are lower than in Abidjan AE=0.73 (0.44, 0.97), possibly reflecting a larger influence of mineral dust.

Table 1. Summary of observations period, number of days of observations (N) per instrument and location. Median and interquartile range for aerosol optical depth (AOD) and Angström exponent (AE).

Site	Type	Latitude	Longitude	period	N	AOD median (IQR)	AE median (IQR)
Lamto	HHC	6°13' N	5° 2' W	Mar. 2006- Mar. 2008	524	0.55 (0.35, 0.80)	0.68 (0.42, 0.96)
Abidjan	CALITOO	5° 20' N	3°59' W	Feb. 2015- Apr. 2017	190	0.55 (0.38, 0.75)	0.73 (0.44, 0.97)
Lamto	CALITOO	6°13' N	5° 2' W	Nov. 2014- Jun. 2016	499	0.47 (0.30, 0.72)	0.59 (0.35, 0.86)
Save	CALITOO	8° 01' N	2° 28' E	Sep. 2015- Oct. 2017	411	0.61 (0.42, 0.86)	0.49 (0.26, 0.73)
Comoe	CALITOO	8° 27' N	3° 28' W	Jan. 2016- Feb. 2017	82	0.66 (0.43, 0.95)	0.33 (0.13, 0.55)
Cotonou	CALITOO	6° 22' N	2° 26' E	Nov. 2014- Jun. 2016	615	0.58 (0.35, 0.86)	0.58 (0.32, 0.89)
Lamto	AERONET	6°13' N	5° 2' W	Jan. 2017- Oct. 2017	35	0.74 (0.59, 0.83)	0.82 (0.58, 1.08)
Ilorin	AERONET	8° 29' N	4° 40' E	Jan. 2014- Oct. 2017	472	0.52 (0.30, 0.89)	0.63 (0.39, 1.00)
Koforidua	AERONET	6° 6' N	0° 6' W	Dec. 2015- Oct. 2017	264	0.54 (0.32, 0.92)	0.78 (0.56, 1.09)

https://doi.org/10.5194/acp-2020-617
Preprint. Discussion started: 11 August 2020


Atmospheric Chemistry and Physics Discussions

3.2 Time series

The daily AODs and AEs for each site and each instrument between 2015 and 2017 (between 2006 and 2008 for HHC) are presented in Figure 2 and 3. A similar seasonal pattern is observed in the different time series. There is an increase in AOD during the main dry season (December to March) and a decrease during the rainy season (April-July). The 2-week smoothing average reveals a high degree of correlation between time series. The correlation coefficient between Cotonou and Lamto time series is R=0.82 and R=0.90 between Cotonou and Koforidua. During the short overlap period in March 2017, the CALITOO and AERONET instruments shows similar AOD values at Lamto station. The Comoé time series is the weakest one with only 82 data points. The 2006-2008 HHC Lamto time series has the same pattern as the one recorded by CALITOO in 2015-2017 and showing two maxima in the dry season, one in December and another one in January-February.

The seasonal pattern for AEs (right side of Figure 3) shows an opposite cycle with lower values in the dry season and higher values during the rainy season. The median AE value during the first half of the year (all site except Comoé) is 0.36 (0.23, 0.62) and 0.69 (0.43, 1.00) during the second half of the year.

AOD in the last quartile (AOD above 0.82) are mostly (72%) observed during the month of December, January and February and are associated with a median AE of 0.44 (0.24, 0.64). While low AODs (first quartile, i.e. below 0.33) are associated to a median AE of 0.89 (0.61, 1.12) and observed between August and October (51% of the observations).

The difference in AOD between the inland and the coastal sites is less than 0.05, with differences up to 0.1 between April and June, the AOD at the coastal stations being higher than inland. AE are higher at the coastal stations than at the inland stations by 0.15 on average.

https://doi.org/10.5194/acp-2020-617
Preprint. Discussion started: 11 August 2020

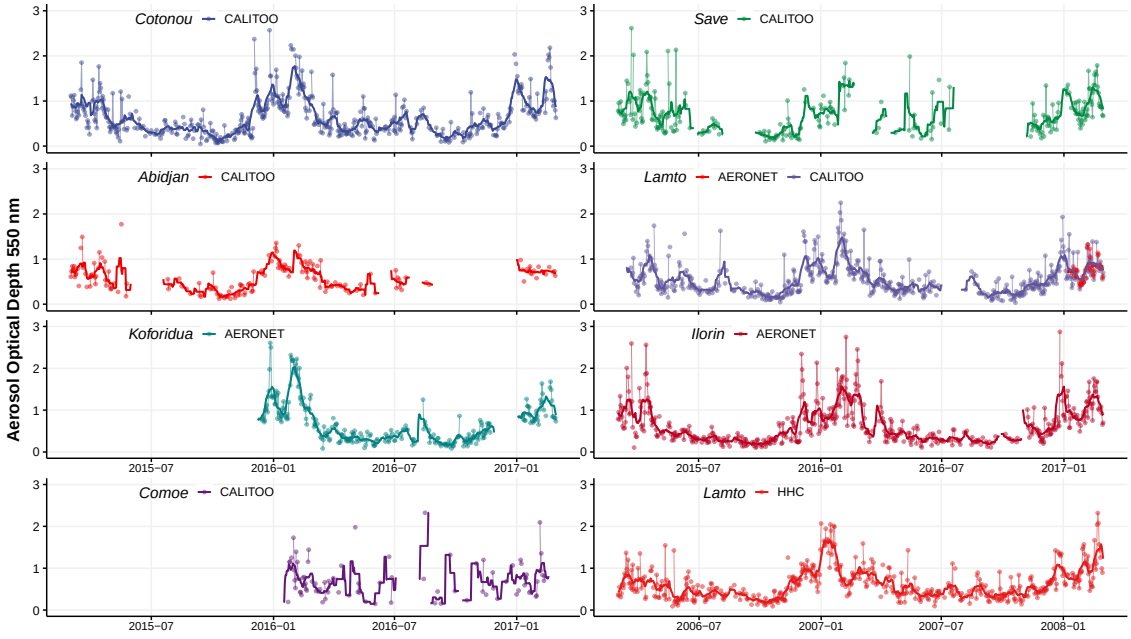

Figure 2. Daily Aerosol Optical Depth at 550 nm. The name of the site and the type of instrument used is given in the legend of each plot. Solid line is a 2-week smoothing average.

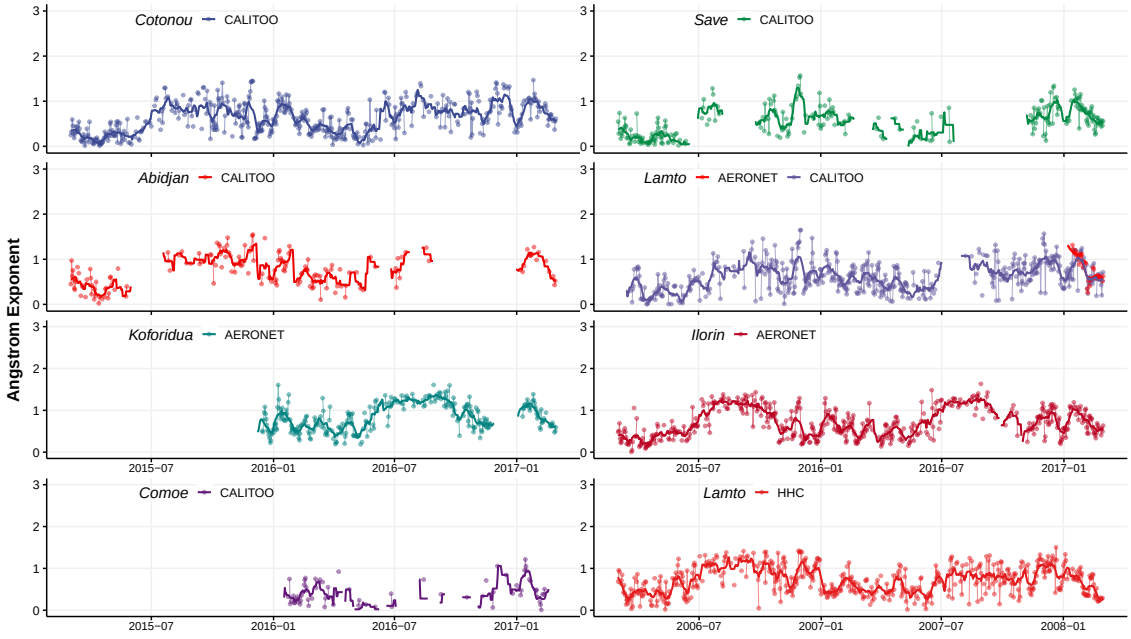

Figure 3. Same as Figure 2 for the visible Angstrom Exponent.

https://doi.org/10.5194/acp-2020-617
Preprint. Discussion started: 11 August 2020

Atmospheric Chemistry and Physics Discussions

3.3 Comparison with MODIS aerosol products

Table 2 gives the statistics of the regressions for each site and per instrument presented in Figure 4. We have then adopted a log-log representation on the scatter plots presented in Figure 4 as the AOD distribution has a significant right skewness (O'Neill et al., 2000). Figure 4 presents also the MODIS expected error (EE, blue lines). Whatever the site is, there is a significant correlation between the MODIS and sun photometer observations. The Pearson correlation coefficient R ranges between 0.75 (Comoé) and 0.94 (Koforidua). For the CALITOO observations, R is between 0.75 and 0.90 (Cotonou). The lowest RMSE are found for the measurements operated using the CALITOO at the coastal sites of Abidjan and Cotonou. The MAPE is on average 30%. The sites in Cotonou and Abdijan are not biased and present a fraction of data falling within the MODIS EE above 60%. All the inland sites are biased and it results in a rather low fraction of data falling within the MODIS expected error.

Table 2. Results of the MODIS and sun photometer AOD comparison by site location and type of instrument indicating the (N) number of data, (R) Pearson correlation coefficient, (RMSE) root mean square error, bias, (MAPE) mean absolute percentage error and (fEE) fraction falling within the MODIS expected error.

site	type	N	R	RMSE	Bias	MAPE(%)	fEE(%)
Savé	CALITOO	295	0.80	0.31	-0.16	33	35
Abidjan	CALITOO	142	0.86	0.14	0.00	21	70
Cotonou	CALITOO	458	0.90	0.21	0.01	29	61
Lamto	CALITOO	235	0.89	0.22	-0.13	28	50
Comoé	CALITOO	53	0.75	0.36	-0.21	29	50
Ilorin	AERONET	327	0.93	0.27	-0.15	30	40
Koforidua	AERONET	177	0.94	0.27	-0.18	27	50
Lamto	AERONET	21	0.86	0.32	-0.29	47	9
Lamto	HHC	219	0.84	0.34	-0.24	33	34

The bias has a seasonal behavior being highest during the dry season between December and March. An underestimation of the MODIS AOD is then observed at maximum in January with an absolute bias of -0.33 (39% in relative) at the inland sites. Sayer et al. (2014) have already pointed out the possible differences in the "Dark Target" and "Deep blue" algorithms. It appears from the Figure 6 in Sayer et al. (2014) that the dry to humid savanna transition zone in sWA is an area where large differences exist in both retrieval techniques during the dry season. Those differences can explain that the "Merge" product used in this study has a large bias during the dry season in the northern part for the inland sites. So the North-South AOD gradient in this area remains difficult to assess based on satellite products.

The histogram of the Sun photometer and MODIS-derived AE are presented in Figure 5. The default values AE=1.5 and AE=1.8 in the MODIS product have been removed (Sayer et al., 2013). The MODIS median AE is biased by 0.32 and the distribution of AE values doesn't follow a normal distribution, whereas the distribution of AE values for the sun photometers does. For all the sites considered in this study and whatever the sun photometer is, the correlation between MODIS and sun

https://doi.org/10.5194/acp-2020-617
Preprint. Discussion started: 11 August 2020

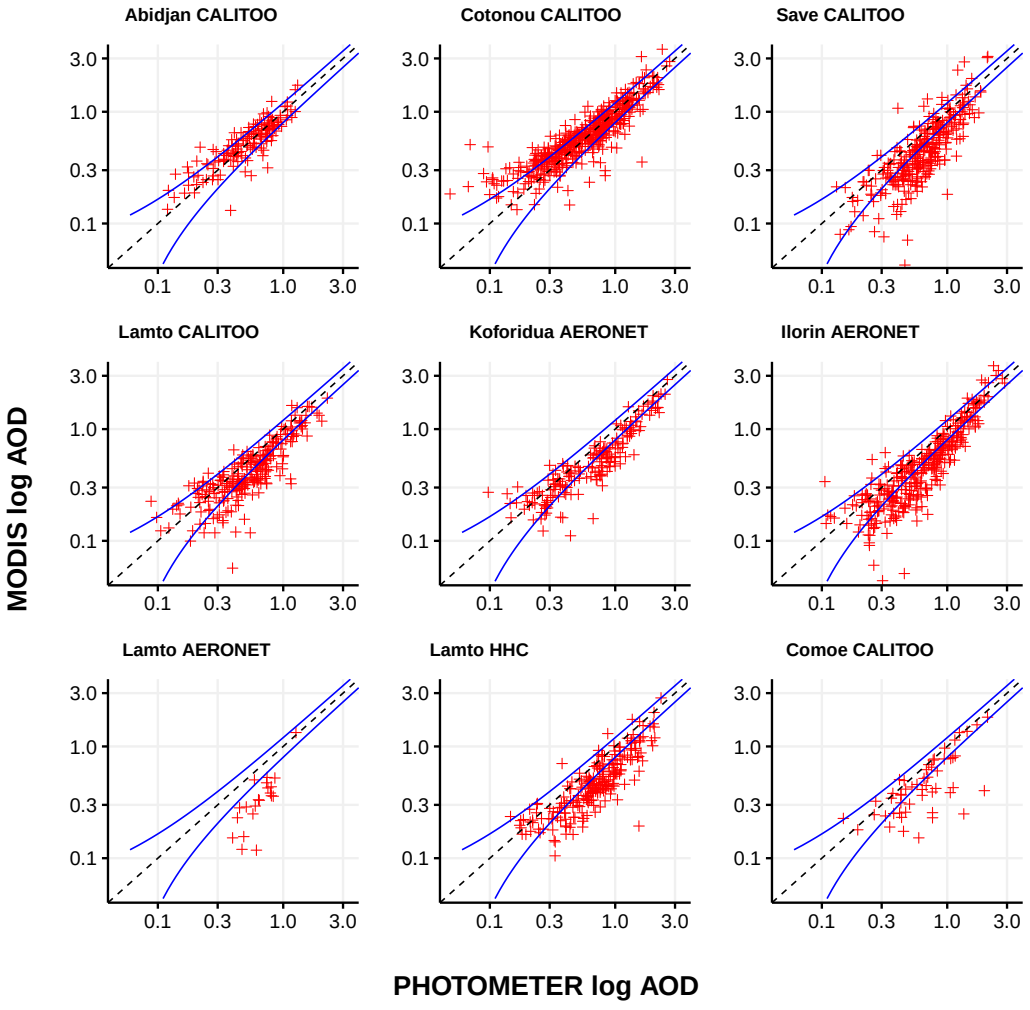

Figure 4. Scatterplots of MODIS versus sun photometer AOD for the 3 types of sun photometers (automatic AERONET, and handheld CALITOO and CIMEL) and different sites (Lamto, Comoé, Savè, Cotonou, Abidjan, Ilorin, Koforidua)

.

photometer AE is non significant. This finding is coherent with the results of Antuña-Marrero et al. (2018) and Sayer et al. (2013).

4 Aerosol type and relationship with surface concentrations

AE depends on the aerosol size distribution and aerosol optical properties (Nakajima et al., 1996; Eck et al., 1999; Holben et al., 2001) and is commonly used to identify aerosol types (Léon et al., 1999; Kaskaoutis et al., 2009; Perrone et al., 2005). Aerosol types having a dominant fraction of their size distribution in the coarse mode, like dust and sea-salt particles, are associated

https://doi.org/10.5194/acp-2020-617
Preprint. Discussion started: 11 August 2020

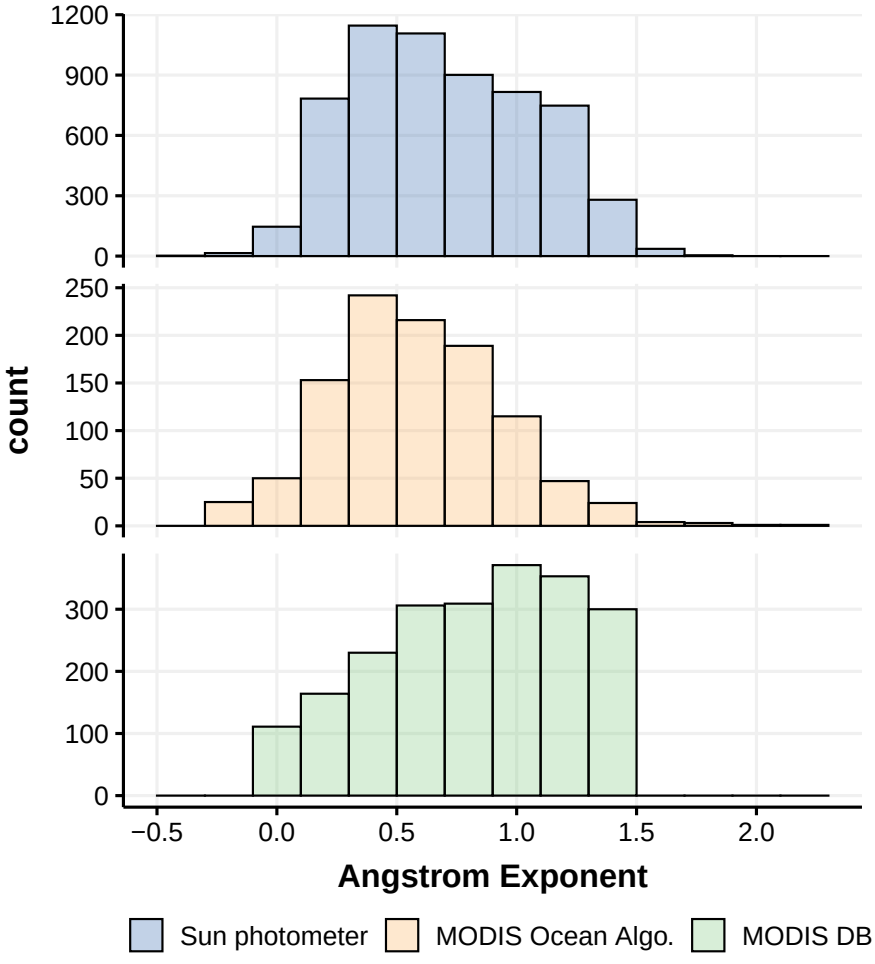

Figure 5. Histogram of Angstrom Exponents for all sun photometer observations and MODIS DB and Ocean algorithms.

with a lower value of AE than aerosol types having a size distribution dominated by the accumulation mode, like secondary and combustion aerosols. The concurrent changes in AOD and AE help to distinguish generic aerosol types in sun photometer time series (Toledano et al., 2007; Verma, 2015). Mineral dust tends to increase atmospheric AOD and decrease AE (Hamonou et al., 1999) while biomass burning events tends to increase both AE and AOD (Eck et al., 2003). The thresholding in AOD and AE for aerosol type identification varies from one site to another and also depends on the distance from aerosol sources upwind the site (Verma, 2015; Benkhalifa et al., 2017).

In this paper we classify the daily observations according to the AE values using a simple statistical analysis. The whole sun photometer dataset is divided into 3 quantiles. The first third corresponds to AE$\leq$0.45 and observations are labelled "coarse dust". The last third corresponds to AE$\geq$0.80 and is labelled "urban-like". The data having 0.45<AE<0.80 falls into a "mixed"

https://doi.org/10.5194/acp-2020-617
Preprint. Discussion started: 11 August 2020


Atmospheric Chemistry and Physics Discussions

category. This rather crude classification enable to identify the main aerosol influence with a significant number of observations in each categories.

Table 3. Percentage of daily observations for each site and by aerosol category considering data falling within the AOD interquartile range and above the last quartile (numbers in brackets).

site	Urban-like	Mixed	Coarse Dust
Abidjan	34.4 (25.6)	37.7 (35.9)	27.9 (38.5)
Comoe	10.9 (3.8)	41.3 (1.5)	47.8 (84.6)
Lamto	37.2 (11.7)	35.7 (32.5)	27.2 (55.8)
Save	22.1 (13.0)	32.8 (30.1)	45.1 (56.9)
Cotonou	34.3 (15.9)	26.3 (35.2)	39.4 (48.9)
Ilorin	28.9 (12.8)	39.3 (32.6)	31.8 (54.6)
Koforidua	46.5 (27.3)	39.5 (55.7)	14.0 (17.0)

Table 3 presents the typology of the sites according to the aforementioned classification. The classification is given for the observations falling within the AOD IQR (see table 1). We also report the percentage of observations having AOD in the last quartile of the AOD distribution to highlight the contribution of the different aerosol types to the aerosol events. As expected the percentage of each catergory for a given site represents roughly one third of the data set. Two sites are less influenced by urban-like aerosols than the others, namely Save and Comoe. For all the sites excepted Koforidua, most of the days showing a large AOD are associated with coarse dust events. Cotonou is also also more influenced bu Coarse Dust (39%) than Abidjan (28%). The northernmost sites are more affected by dust events and the influence of coarse dust on the AOD decreases from North to South and East to West.

As reported by Djossou et al. (2018), the changeover between the monsoon and the harmattan circulation leads to a drastic change in the aerosol type and stratification. The harmattan flow carries continental aerosols in the lowest part of the atmosphere during the long dry winter season. During this period, the days with high AOD are often associated with an increase in the PM2.5 surface concentration. As a consequence, the correlation coefficient between AOD and PM2.5 is the highest during the dry long season (Djossou et al., 2018). Considering the whole dataset of PM2.5 and AOD (weekly basis) measured in Cotonou and Abidjan, the correlation between PM2.5 and AOD is significant with a correlation coeff. R=0.75, (N=105). The correlation can reach R=0.96 (N=6) during aerosol events observed from December 2015 to January 2016 in the heart of the dry season.

The variation in the PM2.5/AOD ratio is estimed as a function of the season and the aerosol type. The data set is divided into 4 periods: the long dry season (Dec.-Mar), the long wet season (Apr.-Jun.) and the short dry (Aug.-Sep.) and short wet season (Oct.-Nov.) Weekly mean AODs are calculated by aerosol category and the PM2.5/AOD ratii are determined from a multilinear regression analysis between the weekly PM2.5 and the AODs. The PM2.5/AOD ratios by aerosol category are presented in Figure 6 as a function of the season and with their respective uncertainties. The PM2.5/AOD ratio ranges between $11 \pm 4\ \mu g/m^3/AOD$ in the short dry season for the Mixed category upto $78 \pm 12\ \mu g/m^3/AOD$ in the short wet season for coarse dust. The uncertainties depends on the occurence of an aerosol category for a given season.

https://doi.org/10.5194/acp-2020-617
Preprint. Discussion started: 11 August 2020

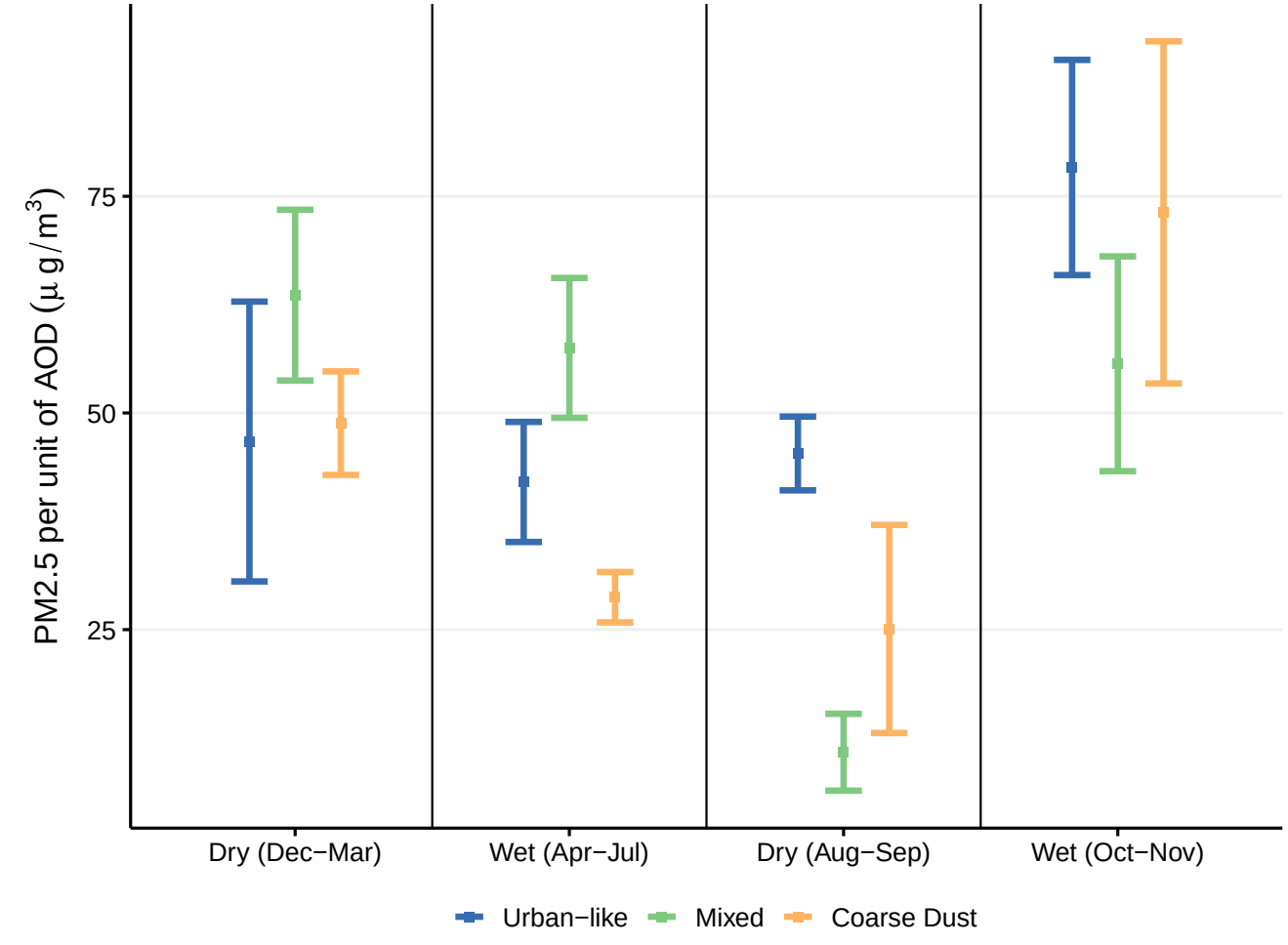

Figure 6. Ratio of PM2.5 to AOD for each of the aerosol types during the long dry (Dec.-Mar) and long wet (Apr.-Jun.) seasons and the short dry (Aug.-Sep.) and short wet (Oct.-Nov.) seasons. Data are collected in Abidjan and Cotonou cities from 2015 to 2017.

The PM2.5/AOD ratio for coarse dust decreases from $49 \pm 6\ \mu g/m^3/AOD$ to $29 \pm 3\ \mu g/m^3/AOD$ between the long dry and long wet season. This change in the ratio reflects the seasonal change in the altitude of coarse dust transport. During the wet (long) season, the air masses are uplifted by the monsoon flow. PM2.5 concentrations remains moderate while AODs are still significant due to aloft transport. Conversely the PM2.5/AOD ratio remains rather constant from the long dry to the short dry season, between $45 \pm 4\ \mu g/m^3/AOD$ and $47 \pm 16\ \mu g/m^3/AOD$. This ratio increases in the short season and reaches $78 \pm 12\ \mu g/m^3/AOD$. This later period shows the largest uncertainties on the estimation of the PM2.5/AOD ratio due to moderate AODs leading to a less accurate regression.

https://doi.org/10.5194/acp-2020-617
Preprint. Discussion started: 11 August 2020

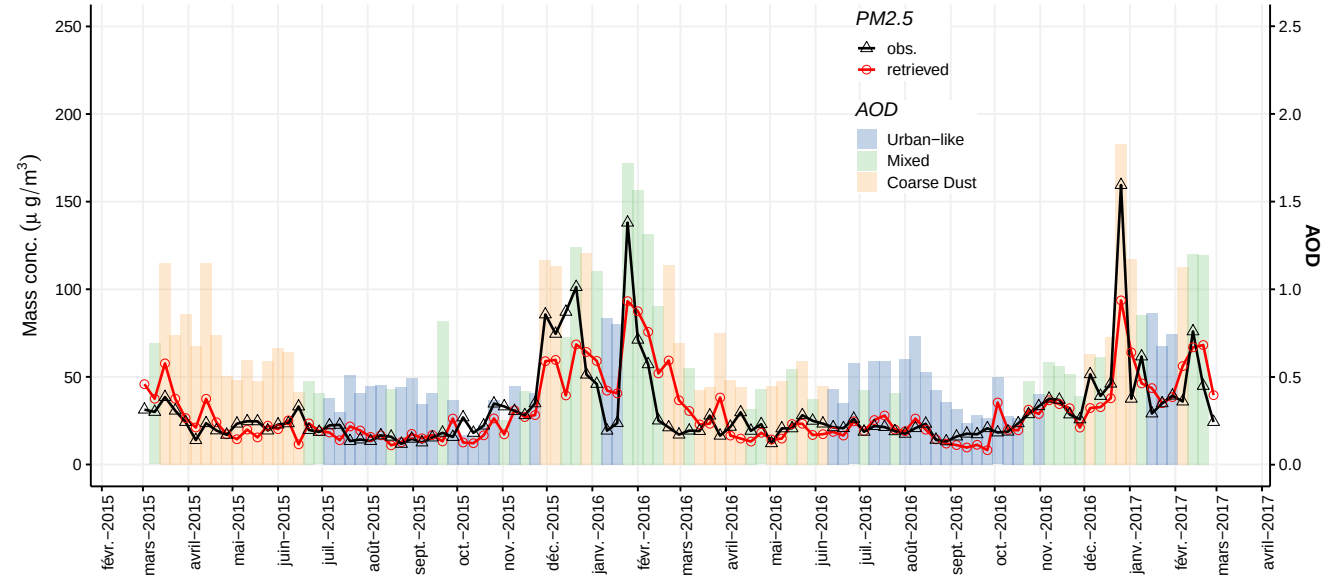

Figure 7. In situ and AOD-derived mean weekly PM2.5 from March 2015 to March 2017 in Abidjan and Cotonou. Vertical color bars give the weakly AOD by aerosol category.

Figure 7 presents the weekly average AODs, satellite-derived and in situ PM2.5 for both Abidjan and Cotonou together. The label attributed to each week corresponds to the dominant aerosol type during the week based on daily AOD. The period from March to May is dominated by the coarse dust type and there is a clear shift to urban-like type in June-July. A second period of coarse dust is observed in December (2015 and 2016) and is associated to a significant increase in both AOD and PM2.5. PM2.5 during the dusty period of December rise close to 100 $\mu g/m^3$. Another sharp increase is observed in February and is associated to the mixed aerosol type. For both years, the two intense periods (December and February) are separeted by an interim period showing moderate PM2.5 and AOD and classified as urban-like aerosols.

On average, satellite-derived PM2.5 are in an excellent agreement with the in situ PM2.5 observations. The MAE is 9.8 $\mu g/m^3$ and the RMSE is 14.6 $\mu g/m^3$. The intense periods are underestimated, e.g. the mean difference between retrieved and observed PM2.5 is -20 $\mu g/m^3$ (-25%) in December 2015. However the satellite-derived concentrations in January and in March are overestimated. The smoothing effect of the weekly concentrations can result from the ajdustment of the regression coefficients on a seasonal basis. Indeed the the mean difference between retrieved and observed PM2.5 during the 2015-2016 period is only 3 $\mu g/m^3$ (6%).

https://doi.org/10.5194/acp-2020-617
Preprint. Discussion started: 11 August 2020

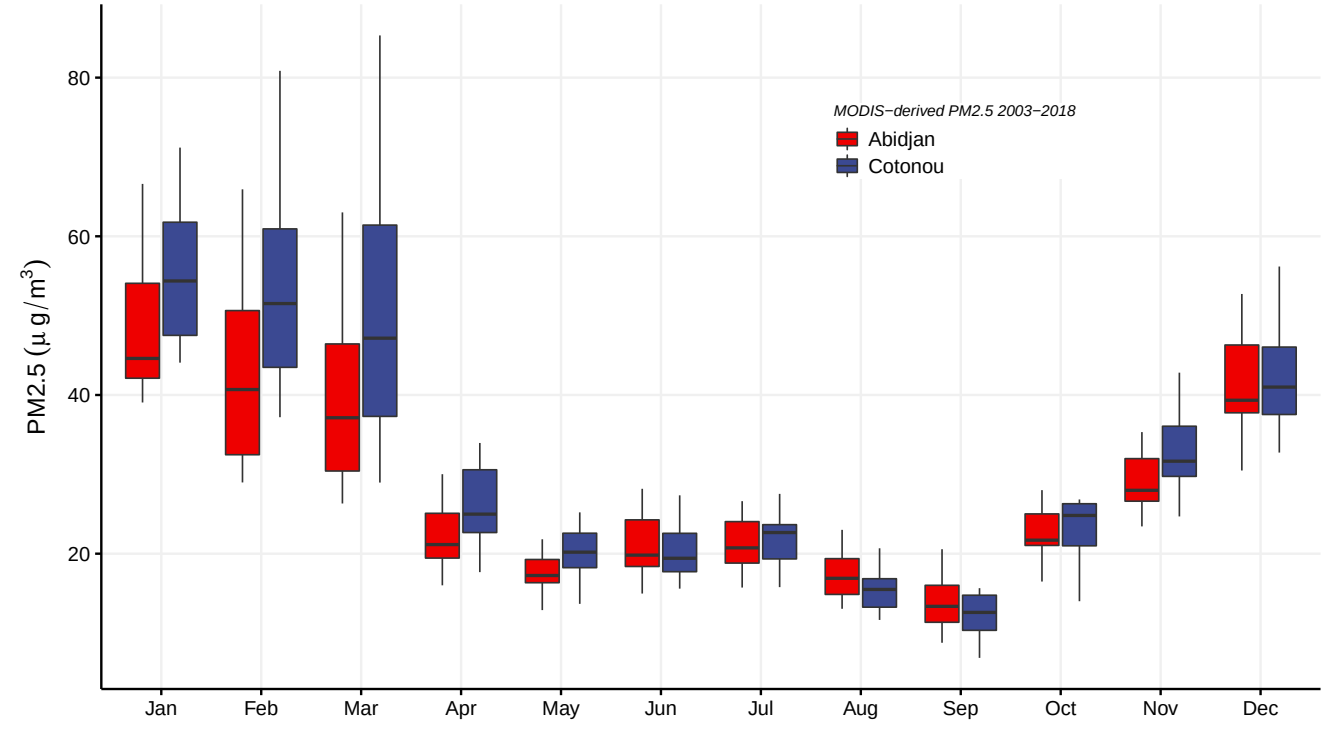

Figure 8. Seasonal cycle of monthly average MODIS-derived PM2.5 in Abidjan and Cotonou cities from 2003 to 2018. Lower and upper hinges correspond to the first and third quartiles. Upper and lower whiskers extend to largest value (respectively lower) no further (respectively at most) 1.5*IQR.

5 Trend in the MODIS-derived PM2.5 time series

We have applied the PM2.5/AOD conversion factors to the daily MODIS AOD observations between 2003 and 2018. The database of daily AOD observations consists in 3170 observations for the area of Abidjan and 3573 for the the area of Cotonou. Daily mean retrieved PM2.5 is 31.4 $\pm$ 19.6 and 34.5 $\pm$ 24 $\mu g/m^3$ in Abidjan and Cotonou, respectively. More than 90% of daily observations are above 10 $\mu g/m^3$ for both cities. Maximum are observed as high as 300 $\mu g/m^3$ during dust event in winter 2010 in Abidjan.

The MODIS-derived PM2.5 monthly mean seasonal cycle is given in Figure 8 for both cities. A first period is observed between December to March when concentrations are at highest. During this period, the overall median PM2.5 value is 43 $\mu g/m^3$, concentrations in Cotonou being 20% higher than in Abdijan. A second period is observed between April and September showing median PM2.5 around 20 $\mu g/m^3$ for both cities. The third period corresponds to steady increase in PM2.5 between September to the December. PM2.5 concentrations are then multiplied by a factor of about 3 in 4 months.

https://doi.org/10.5194/acp-2020-617
Preprint. Discussion started: 11 August 2020

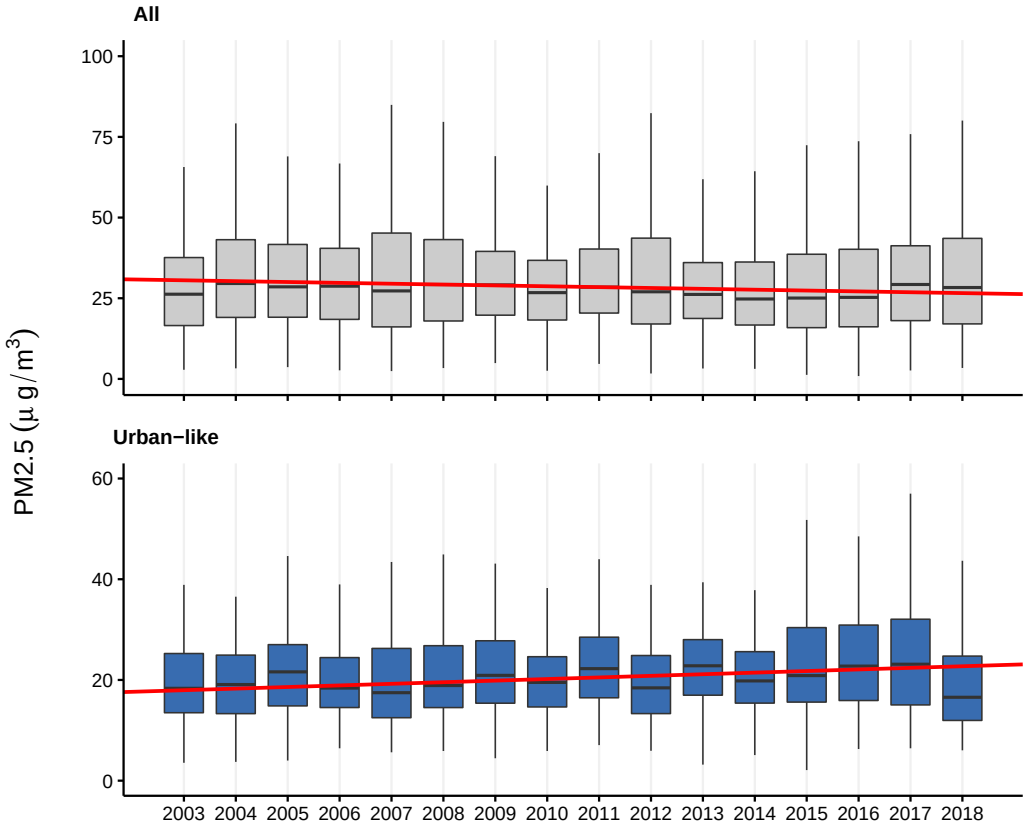

Figure 9. PM2.5 annual mean for Abidjan and Cotonou from 2003 to 2018. (top) all type of aerosols, (bottom) urban-like type only.

The percentage of daily observations falling in the coarse dust aerosol category is about 60% from January to April. The urban-like category represent 10% of the daily observations during the same period. The percentage of observations identified as coarse dust decreases from April to July down to 20% on average. From July to October, the urban-like category represents 50% of the observations.

There is no obvious trend in the MODIS-derived PM2.5 annual time series. Mann-Kendall's trend test on annual median values is not significant (tau=-0.31, p-value=0.11). Figure 8 represents the annual boxplots of daily concentrations between 2003 and 2018. The annual boxplots considering only the days during which the AOD belongs to the urban-like aerosol category are also plotted on Figure 8. The drop in the concentration in 2018 is not clearly explained. Over the period 2003-2017, we observe a significant increasing trend in the annual values (tau=0.50, p-value=0.01). The Thiel-Sen's slope over 2003-2017 is 0.32 with an 95% confidence interval of (0.11, 0.51). This weak relatively weak trend leads to an increase of about $5 \pm 3\ \mu g/m^3$ over 15 years (25% in relative).

https://doi.org/10.5194/acp-2020-617
Preprint. Discussion started: 11 August 2020


Atmospheric Chemistry and Physics Discussions

6 Conclusions

An increase in the anthropogenic emission of atmospheric pollutants is expected as a result of the massive urbanization of the Gulf of Guinea. The scarcity of ground-based observations in sWA is still a limiting factor for a comprehensive understanding of the short-time trend over growing African cities. Moreover, the large influence of natural aerosol emission in sWA produces a complex mixing of particles in the cities atmosphere. In this paper, sun photometer and satellite observations have been used to characterize the magnitude and seasonal behaviour of the aerosol optical depth in sWA. We have set up a small network of lightweight handheld sun photometers, that provides an unprecedented data set on the AOD over sWA between 2015 and 2017. This data set was complemented by additional measurements from AERONET data and observations obtained during a previous campaign in 2006 in Côte d'Ivoire. The comparison of our observations with the MODIS satellite observations shows that the satellite AOD derived in the vicinity of the coastal conurbation are excellent, while there is a possible negative bias for the retrievals farther inland, that must be further investigated.

A basic classification using the AOD spectral dependency reveals the large impact of the advection of mineral dust on the AOD seasonal cycle. Dust impacts the cities of the northern part of the gulf of Guinea (namely Abidjan and Cotonou in the present study) from December to May and brings the largest AODs during the months of December and February.

Weekly surface PM2.5 in Abidjan and Cotonou and daily AOD observations were used to estimate a set of AOD to PM2.5 conversion coefficients that accounts for the aerosol typing and the season. Despite a good agreement for most of the year, the retrieved PM2.5 underestimates the actual concentrations during the large events in the dry season. Reversely the PM2.5 are overestimated in early march as a consequence of the shift in altitude of the Harmattan wind. Nonetheless the seasonal variability of the PM2.5 concentrations is in a good agreement with the actual ones. The PM2.5/AOD conversion coefficients are applied to the MODIS time series from 2003 to 2018. A significant increase is observed during the 2003-2017 period in PM2.5 during the days falling in the urban-like aerosol category. The trend corresponds to an increase of 25% over 15 years.

There are several mechanisms that can lead to the increase in the anthropogenic PM2.5 concentrations. Combustion sources are subject to an increase in sWA as well as for the rest of Africa, e.g. organic carbon emissions are multiplied by a factor between 1.5 and 3.0 over 2005-2030 Liousse et al. (2014). However recent studies show a decrease in gas flaring emissions in the Niger delta area (Deetz and Vogel, 2017; Doumbia et al., 2019), the conurbations of the Gulf of Guinea are directly under the influence of such emission the year-to-year variability of such emissions has to be investigated The increase found in the urban-like PM2.5 corresponds to an average annual growth rate of 1.48% in agreement with the lower bound of the emission scenarii. However there is no evidence that the observed trend in our data is linked to an increase in the local city emissions. The phenomena can also be linked to the advection of biomass burning byproducts from central Africa and crossing the gulf of Guinea resulting from the zonal transport (Menut et al., 2018; Flamant et al., 2018). In addition to satellite data, unraveling the causes and consequences of the changes in aerosol concentrations in this area of the world that is under a significant anthropogenic pressure requires sustaining long-term in situ observations of the aerosol concentrations and chemical composition.

https://doi.org/10.5194/acp-2020-617
Preprint. Discussion started: 11 August 2020

Atmospheric Chemistry and Physics Discussions

Data availability. Handheld sun photometer are available at http://baobab.sedoo.fr/. AERONET sun photometer data are available at https://aeronet.gsfc.nasa.gov/. MODIS AQUA data are available at http://giovanni.gsfc.nasa.gov

Acknowledgements. The research leading to these results has received funding from the European Union 7th Framework Programme (FP7/2007-2013) under Grant Agreement no. 603502 (EU project DACCIWA: Dynamics-aerosol-chemistry-cloud interactions in West Africa). The authors greatly thank all the operators who contribute to the acquisition of handheld sun photometer observations at Lamto geophysical station, CEG Dantokpa and CEG Savè. We acknowledge the AERONET and PHOTONS sun-photometer networks their staff, and the PI of the sites for their work to produce the dataset used in this study (http://aeronet.gsfc.nasa.gov/). Handheld CIMEL data were processed by I. Jankowiak (LOA, Université Lille 1).

https://doi.org/10.5194/acp-2020-617
Preprint. Discussion started: 11 August 2020

Atmospheric Chemistry and Physics Discussions

References

Adetunji, J., McGregor, J., and Ong, C. K.: Harmattan Haze, Weather, 34, 430–436, https://doi.org/10.1002/j.1477-8696.1979.tb03389.x, 1979.

Angström, A.: Techniques of Determinig the Turbidity of the Atmosphere, Tellus, 13, 214–223, https://doi.org/10.1111/j.2153-3490.1961.tb00078.x, 1961.

Antuña-Marrero, J. C., Cachorro Revilla, V., García Parrado, F., de Frutos Baraja, A., Rodríguez Vega, A., Mateos, D., Estevan Arredondo, R., and Toledano, C.: Comparison of Aerosol Optical Depth from Satellite (MODIS), Sun Photometer and Broadband Pyrheliometer Ground-Based Observations in Cuba, Atmospheric Meas. Tech., 11, 2279–2293, https://doi.org/10.5194/amt-11-2279-2018, 2018.

Basart, S., Pérez, C., Cuevas, E., Baldasano, J. M., and Gobbi, G. P.: Aerosol Characterization in Northern Africa, Northeastern Atlantic, Mediterranean Basin and Middle East from Direct-Sun AERONET Observations, Atmos. Chem. Phys, 9, 8265–8282, 2009.

Benedetti, A., Morcrette, J.-J., Boucher, O., Dethof, A., Engelen, R. J., Fisher, M., Flentje, H., Huneeus, N., Jones, L., Kaiser, J. W., Kinne, S., Mangold, A., Razinger, M., Simmons, A. J., and Suttie, M.: Aerosol Analysis and Forecast in the European Centre for Medium-Range Weather Forecasts Integrated Forecast System: 2. Data Assimilation, J. Geophys. Res., 114, https://doi.org/10.1029/2008JD011115, 2009.

Benkhalifa, J., Léon, J. F., and Chaabane, M.: Aerosol Optical Properties of Western Mediterranean Basin from Multi-Year AERONET Data, J. Atmos. Sol. Terr. Phys., 164, 222–228, https://doi.org/10.1016/j.jastp.2017.08.029, 2017.

Boers, R., van Weele, M., van Meijgaard, E., Savenije, M., Siebesma, A. P., Bosveld, F., and Stammes, P.: Observations and Projections of Visibility and Aerosol Optical Thickness (1956–2100) in the Netherlands: Impacts of Time-Varying Aerosol Composition and Hygroscopicity, Environ. Res. Lett., 10, 015 003, https://doi.org/10.1088/1748-9326/10/1/015003, 2015.

Boucher, O., Randall, D., Artaxo, P., Bretherton, C., Feingold, G., Forster, P., Kerminen, V.-M., Kondo, Y., Liao, H., Lohmann, U., et al.: Clouds and Aerosols, in: Climate Change 2013: The Physical Science Basis. Contribution of Working Group I to the Fifth Assessment Report of the Intergovernmental Panel on Climate Change, pp. 571–657, Cambridge University Press, 2013.

Deetz, K. and Vogel, B.: Development of a New Gas-Flaring Emission Dataset for Southern West Africa, Geoscientific Model Development, 10, 1607–1620, https://doi.org/10.5194/gmd-10-1607-2017, 2017.

Djossou, J., Léon, J.-F., Akpo, A. B., Liousse, C., Yoboué, V., Bedou, M., Bodjrenou, M., Chiron, C., Galy-Lacaux, C., Gardrat, E., Abbey, M., Keita, S., Bahino, J., Touré N'Datchoh, E., Ossohou, M., and Awanou, C. N.: Mass Concentration, Optical Depth and Carbon Composition of Particulate Matter in the Major Southern West African Cities of Cotonou (Benin) and Abidjan (Côte d'Ivoire), Atmos. Chem. Phys., 18, 6275–6291, https://doi.org/10.5194/acp-18-6275-2018, 2018.

van Donkelaar, A., Martin, R. V., Brauer, M., Hsu, N. C., Kahn, R. A., Levy, R. C., Lyapustin, A., Sayer, A. M., and Winker, D. M.: Global Estimates of Fine Particulate Matter Using a Combined Geophysical-Statistical Method with Information from Satellites, Models, and Monitors, Environmental Science & Technology, 50, 3762–3772, https://doi.org/10.1021/acs.est.5b05833, 2016.

Doumbia, E. H. T., Liousse, C., Keita, S., Granier, L., Granier, C., Elvidge, C. D., Elguindi, N., and Law, K.: Flaring Emissions in Africa: Distribution, Evolution and Comparison with Current Inventories, Atmospheric Environment, 199, 423–434, https://doi.org/10.1016/j.atmosenv.2018.11.006, 2019.

Eck, T. F., Holben, B. N., Reid, J. S., Dubovik, O., Smirnov, A., O'Neill, N. T., Slutsker, I., and Kinne, S.: Wavelength Dependence of the Optical Depth of Biomass Burning, Urban, and Desert Dust Aerosols, J. Geophys. Res., 104, 31 333, https://doi.org/10.1029/1999JD900923, 1999.

https://doi.org/10.5194/acp-2020-617
Preprint. Discussion started: 11 August 2020

Atmospheric Chemistry and Physics Discussions

Eck, T. F., Holben, B. N., Ward, D. E., Mukelabai, M. M., Dubovik, O., Smirnov, A., Schafer, J. S., Hsu, N. C., Piketh, S. J., Queface, A., Roux, J. L., Swap, R. J., and Slutsker, I.: Variability of Biomass Burning Aerosol Optical Characteristics in Southern Africa during the SAFARI 2000 Dry Season Campaign and a Comparison of Single Scattering Albedo Estimates from Radiometric Measurements, J. Geophys. Res.: Atmospheres, 108, 8477, https://doi.org/10.1029/2002JD002321, 2003.

Flamant, C., Deroubaix, A., Chazette, P., Brito, J., Gaetani, M., Knippertz, P., Fink, A. H., de Coetlogon, G., Menut, L., Colomb, A., Denjean, C., Meynadier, R., Rosenberg, P., Dupuy, R., Dominutti, P., Duplissy, J., Bourrianne, T., Schwarzenboeck, A., Ramonet, M., and Totems, J.: Aerosol Distribution in the Northern Gulf of Guinea: Local Anthropogenic Sources, Long-Range Transport, and the Role of Coastal Shallow Circulations, Atmospheric Chemistry and Physics, 18, 12 363–12 389, https://doi.org/https://doi.org/10.5194/acp-18-12363-2018, 2018.

Giles, D. M., Sinyuk, A., Sorokin, M. G., Schafer, J. S., Smirnov, A., Slutsker, I., Eck, T. F., Holben, B. N., Lewis, J. R., Campbell, J. R., Welton, E. J., Korkin, S. V., and Lyapustin, A. I.: Advancements in the Aerosol Robotic Network (AERONET) Version 3 Database – Automated near-Real-Time Quality Control Algorithm with Improved Cloud Screening for Sun Photometer Aerosol Optical Depth (AOD) Measurements, Atmospheric Measurement Techniques, 12, 169–209, https://doi.org/https://doi.org/10.5194/amt-12-169-2019, 2019.

Gupta, P. and Christopher, S. A.: Particulate Matter Air Quality Assessment Using Integrated Surface, Satellite, and Meteorological Products: Multiple Regression Approach, J. Geophys. Res., 114, https://doi.org/10.1029/2008JD011496, 2009.

Hamonou, E., Chazette, P., Balis, D., Dulac, F., Schneider, X., Galani, E., Ancellet, G., and Papayannis, A.: Characterization of the Vertical Structure of Saharan Dust Export to the Mediterranean Basin, J. Geophys. Res.: Atmospheres, 104, 22 257–22 270, https://doi.org/10.1029/1999JD900257, 1999.

Hoff, R. M. and Christopher, S. A.: Remote Sensing of Particulate Pollution from Space: Have We Reached the Promised Land?, Journal of the Air & Waste Manage. (Oxford) Association, 59, 645–675, https://doi.org/10.3155/1047-3289.59.6.645, 2009.

Holben, B. N., Eck, T. F., Slutsker, I., Tanre, D., Buis, J. P., Setzer, A., Vermote, E., Reagan, J. A., Kaufman, Y. J., Nakajima, T., et al.: AERONET—A Federated Instrument Network and Data Archive for Aerosol Characterization, Remote Sens. Environ., 66, 1–16, 1998.

Holben, B. N., Tanre, D., Smirnov, A., Eck, T. F., Slutsker, I., Abuhassan, N., Newcomb, W. W., Schafer, J. S., Chatenet, B., Lavenu, F., et al.: An Emerging Ground-Based Aerosol Climatology: Aerosol Optical Depth from AERONET, J. Geophys. Res.: Atmospheres (1984–2012), 106, 12 067–12 097, 2001.

Janicot, S.: Spatiotemporal Variability of West African Rainfall. Part II: Associated Surface and Airmass Characteristics, J. Climate, 5, 499–511, https://doi.org/10.1175/1520-0442(1992)005<0499:SVOWAR>2.0.CO;2, 1992.

Kacenelenbogen, M., Léon, J.-F., Chiapello, I., and Tanré, D.: Characterization of Aerosol Pollution Events in France Using Ground-Based and POLDER-2 Satellite Data, Atmos. Chem. Phys., 6, 4843–4849, 2006.

Kamarul Zaman, N. A. F., Kanniah, K. D., and Kaskaoutis, D. G.: Estimating Particulate Matter Using Satellite Based Aerosol Optical Depth and Meteorological Variables in Malaysia, Atmospheric Research, 193, 142–162, https://doi.org/10.1016/j.atmosres.2017.04.019, 2017.

Kaskaoutis, D. G., Badarinath, K. V. S., Kharol, S. K., Sharma, A. R., and Kambezidis, H. D.: Variations in the Aerosol Optical Properties and Types over the Tropical Urban Site of Hyderabad, India, J. Geophys. Res.: Atmospheres, 114, https://doi.org/10.1029/2009JD012423, 2009.

Kaufman, Y. J., Tanré, D., Gordon, H. R., Nakajima, T., Lenoble, J., Frouin, R., Grassl, H., Herman, B. M., King, M. D., and Teillet, P. M.: Passive Remote Sensing of Tropospheric Aerosol and Atmospheric Correction for the Aerosol Effect, J. Geophys. Res.: Atmospheres (1984–2012), 102, 16 815–16 830, 1997.

https://doi.org/10.5194/acp-2020-617
Preprint. Discussion started: 11 August 2020

Atmospheric Chemistry and Physics Discussions

Kaufman, Y. J., Tanré, D., and Boucher, O.: A Satellite View of Aerosols in the Climate System, Nature, 419, 215–223, https://doi.org/10.1038/nature01091, 2002.

Knippertz, P., Evans, M. J., Field, P. R., Fink, A. H., Liousse, C., and Marsham, J. H.: The Possible Role of Local Air Pollution in Climate Change in West Africa, Nature Climate Change, 5, 815–822, https://doi.org/10.1038/nclimate2727, 2015.

Koren, I., Kaufman, Y. J., Washington, R., Todd, M. C., Rudich, Y., Martins, J. V., and Rosenfeld, D.: The Bodele Depression: A Single Spot in the Sahara That Provides Most of the Mineral Dust to the Amazon Forest, Environ. Res. Lett., 1, 014 005, https://doi.org/10.1088/1748-9326/1/1/014005, 2006.

Lélé, M. I. and Lamb, P. J.: Variability of the Intertropical Front (ITF) and Rainfall over the West African Sudan-Sahel Zone, J. Climate, 23, 3984–4004, https://doi.org/10.1175/2010JCLI3277.1, 2010.

Léon, J.-F., Chazette, P., and Dulac, F.: Retrieval and Monitoring of Aerosol Optical Thickness over an Urban Area by Spaceborne and Ground-Based Remote Sensing, Appl. Opt., 38, 6918–6926, 1999.

Léon, J.-F., Derimian, Y., Chiapello, I., Tanré, D., Podvin, T., Chatenet, B., Diallo, A., and Deroo, C.: Aerosol Vertical Distribution and Optical Properties over M'Bour (16.96° W; 14.39° N), Senegal from 2006 to 2008, Atmos. Chem. Phys., 9, 9249–9261, 2009.

Levy, R. C., Remer, L. A., Kleidman, R. G., Mattoo, S., Ichoku, C., Kahn, R., and Eck, T. F.: Global Evaluation of the Collection 5 MODIS Dark-Target Aerosol Products over Land, Atmos. Chem. Phys., 10, 10 399–10 420, https://doi.org/10.5194/acp-10-10399-2010, 2010.

Levy, R. C., Mattoo, S., Munchak, L. A., Remer, L. A., Sayer, A. M., Patadia, F., and Hsu, N. C.: The Collection 6 MODIS Aerosol Products over Land and Ocean, Atmospheric Meas. Tech., 6, 2989–3034, https://doi.org/10.5194/amt-6-2989-2013, 2013.

Liousse, C., Guillaume, B., Grégoire, J. M., Mallet, M., Galy, C., Pont, V., Akpo, A., Bedou, M., Castéra, P., Dungall, L., Gardrat, E., Granier, C., Konaré, A., Malavelle, F., Mariscal, A., Mieville, A., Rosset, R., Serça, D., Solmon, F., Tummon, F., Assamoi, E., Yoboué, V., and Van Velthoven, P.: Updated African Biomass Burning Emission Inventories in the Framework of the AMMA-IDAF Program, with an Evaluation of Combustion Aerosols, Atmos. Chem. Phys., 10, 9631–9646, https://doi.org/10.5194/acp-10-9631-2010, 2010.

Liousse, C., Assamoi, E., Criqui, P., Granier, C., and Rosset, R.: Explosive Growth in African Combustion Emissions from 2005 to 2030, Environ. Res. Lett., 9, 035 003, https://doi.org/10.1088/1748-9326/9/3/035003, 2014.

Lynch, P., Reid, J. S., Westphal, D. L., Zhang, J., Hogan, T. F., Hyer, E. J., Curtis, C. A., Hegg, D. A., Shi, Y., Campbell, J. R., Rubin, J. I., Sessions, W. R., Turk, F. J., and Walker, A. L.: An 11-Year Global Gridded Aerosol Optical Thickness Reanalysis (v1.0) for Atmospheric and Climate Sciences, Geosci. Model Dev., 9, 1489–1522, https://doi.org/10.5194/gmd-9-1489-2016, 2016.

Ma, Z., Hu, X., Sayer, A. M., Levy, R., Zhang, Q., Xue, Y., Tong, S., Bi, J., Huang, L., and Liu, Y.: Satellite-Based Spatiotemporal Trends in PM2.5 Concentrations: China, 2004–2013, Environ. Health Perspect., 124, https://doi.org/10.1289/ehp.1409481, 2015.

Mallet, M., Pont, V., Liousse, C., Gomes, L., Pelon, J., Osborne, S., Haywood, J., Roger, J. C., Dubuisson, P., Mariscal, A., Thouret, V., and Goloub, P.: Aerosol Direct Radiative Forcing over Djougou (Northern Benin) during the African Monsoon Multidisciplinary Analysis Dry Season Experiment (Special Observation Period-0), Journal of Geophysical Research, 113, https://doi.org/10.1029/2007JD009419, 2008.

Menut, L., Flamant, C., Turquety, S., Deroubaix, A., Chazette, P., and Meynadier, R.: Impact of Biomass Burning on Pollutant Surface Concentrations in Megacities of the Gulf of Guinea, Atmos. Chem. Phys., 18, 2687–2707, https://doi.org/https://doi.org/10.5194/acp-18-2687-2018, 2018.

Nakajima, T., Hayasaka, T., Higurashi, A., Hashida, G., Moharram-Nejad, N., Najafi, Y., and Valavi, H.: Aerosol Optical Properties in the Iranian Region Obtained by Ground-Based Solar Radiation Measurements in the Summer Of 1991, J. Appl. Meteorol., 35, 1265–1278, https://doi.org/10.1175/1520-0450(1996)035<1265:AOPITI>2.0.CO;2, 1996.

https://doi.org/10.5194/acp-2020-617
Preprint. Discussion started: 11 August 2020

Atmospheric Chemistry and Physics Discussions

O'Neill, N., Ignatov, A., Holben, B. N., and Eck, T. F.: The Lognormal Distribution as a Reference for Reporting Aerosol Optical Depth Statistics; Empirical Tests Using Multi-Year, Multi-Site AERONET Sunphotometer Data, Geophys. Res. Lett., 27, 3333–3336, https://doi.org/10.1029/2000GL011581, 2000.

Perrone, M., Santese, M., Tafuro, A., Holben, B., and Smirnov, A.: Aerosol Load Characterization over South–East Italy for One Year of AERONET Sun-Photometer Measurements, Atmos. Res., 75, 111–133, https://doi.org/10.1016/j.atmosres.2004.12.003, 2005.

Porter, J. N., Miller, M., Pietras, C., and Motell, C.: Ship-Based Sun Photometer Measurements Using Microtops Sun Photometers, J. Atmos. Oceanic Technol., 18, 765–774, 2001.

Prospero, J., Savoie, D., Carlson, T., and Nees, R.: Saharan Aerosol Transport by Means of Atmospheric Turbidity Measurements, in: Saharan Dust Mobilization, Transport, Deposition, vol. 14, chap. 8, pp. 171–186, edited by John Wiley, San Diego, Calif., 1979.

Redelsperger, J.-L., Thorncroft, C. D., Diedhiou, A., Lebel, T., Parker, D. J., and Polcher, J.: African Monsoon Multidisciplinary Analysis: An International Research Project and Field Campaign, Bull. Amer. Meteor. Soc., 87, 1739–1746, https://doi.org/10.1175/BAMS-87-12-1739, 2006.

Remer, L. A., Kaufman, Y. J., Tanré, D., Mattoo, S., Chu, D. A., Martins, J. V., Li, R.-R., Ichoku, C., Levy, R. C., Kleidman, R. G., Eck, T. F., Vermote, E., and Holben, B. N.: The MODIS Aerosol Algorithm, Products, and Validation, J. Atmos. Sci., 62, 947–973, https://doi.org/10.1175/JAS3385.1, 2005.

Remer, L. A., Kleidman, R. G., Levy, R. C., Kaufman, Y. J., Tanré, D., Mattoo, S., Martins, J. V., Ichoku, C., Koren, I., Yu, H., and Holben, B. N.: Global Aerosol Climatology from the MODIS Satellite Sensors, J. Geophys. Res., 113, https://doi.org/10.1029/2007JD009661, 2008.

Sayer, A. M., Hsu, N. C., Bettenhausen, C., and Jeong, M.-J.: Validation and Uncertainty Estimates for MODIS Collection 6 "Deep Blue" Aerosol Data, J. Geophys. Res.: Atmospheres, 118, 7864–7872, https://doi.org/10.1002/jgrd.50600, 2013.

Sayer, A. M., Munchak, L. A., Hsu, N. C., Levy, R. C., Bettenhausen, C., and Jeong, M.-J.: MODIS Collection 6 Aerosol Products: Comparison between Aqua's e-Deep Blue, Dark Target, and "Merged" Data Sets, and Usage Recommendations, J. Geophys. Res.: Atmospheres, 119, 13, 965–13, 989, https://doi.org/10.1002/2014JD022453, 2014.

Schepanski, K., Tegen, I., and Macke, A.: Saharan Dust Transport and Deposition towards the Tropical Northern Atlantic, Atmos. Chem. Phys., 9, 1173–1189, https://doi.org/10.5194/acp-9-1173-2009, 2009.

Schmid, B. and Wehrli, C.: Comparison of Sun Photometer Calibration by Use of the Langley Technique and the Standard Lamp, Appl. Opt., 34, 4500, https://doi.org/10.1364/AO.34.004500, 1995.

Smirnov, A.: Diurnal Variability of Aerosol Optical Depth Observed at AERONET (Aerosol Robotic Network) Sites, Geophys. Res. Lett., 29, https://doi.org/10.1029/2002GL016305, 2002.

Smirnov, A., Holben, B. N., Eck, T. F., Dubovik, O., and Slutsker, I.: Cloud-Screening and Quality Control Algorithms for the AERONET Database, Remote Sens. Environ., 73, 337–349, https://doi.org/10.1016/S0034-4257(00)00109-7, 2000.

Soufflet, V., Devaux, C., and Tanré, D.: Modified Langley Plot Method for Measuring the Spectral Aerosol Optical Thickness and Its Daily Variations, Appl. Opt., 31, 2154, https://doi.org/10.1364/AO.31.002154, 1992.

Tanré, D., Deschamps, P. Y., Devaux, C., and Herman, M.: Estimation of Saharan Aerosol Optical Thickness from Blurring Effects in Thematic Mapper Data, J. Geophys. Res.: Atmospheres, 93, 15 955–15 964, https://doi.org/10.1029/JD093iD12p15955, 1988.

Todd, M. C., Washington, R., Martins, J. V., Dubovik, O., Lizcano, G., M'Bainayel, S., and Engelstaedter, S.: Mineral Dust Emission from the Bodélé Depression, Northern Chad, during BoDEx 2005, J. Geophys. Res., 112, https://doi.org/10.1029/2006JD007170, 2007.

https://doi.org/10.5194/acp-2020-617
Preprint. Discussion started: 11 August 2020

Toledano, C., Cachorro, V. E., Berjon, A., de Frutos, A. M., Sorribas, M., de la Morena, B. A., and Goloub, P.: Aerosol Optical Depth and Ångström Exponent Climatology at El Arenosillo AERONET Site (Huelva, Spain), Quart. J. Roy. Meteor. Soc., 133, 795–807, https://doi.org/10.1002/qj.54, 2007.

Verma, S.: A New Classification of Aerosol Sources and Types as Measured over Jaipur, India, Aerosol Air Qual. Res., 2015, https://doi.org/10.4209/aaqr.2014.07.0143, 2015.

Volz, F.: Photometer Mit Selen-Photoelement Zur Spektralen Messung Der Sonnenstrahlung Und Zur Bestimmung Der Wellenlängenabhängigkeit Der Dunsttrübung, Archiv für Meteorologie, Geophysik und Bioklimatologie, Serie B, 10, 100–131, https://doi.org/10.1007/BF02243122, 1959.

Volz, F. E.: Economical Multispectral Sun Photometer for Measurements of Aerosol Extinction from 0.44 Mm to 1.6 Mm and Precipitable Water, Appl. Opt., 13, 1732–1733, 1974.

Washington, R.: Atmospheric Controls on Mineral Dust Emission from the Bodélé Depression, Chad: The Role of the Low Level Jet, Geophys. Res. Lett., 32, https://doi.org/10.1029/2005GL023597, 2005.

Yahi, H., Marticorena, B., Thiria, S., Chatenet, B., Schmechtig, C., Rajot, J. L., and Crepon, M.: Statistical Relationship between Surface PM10 Concentration and Aerosol Optical Depth over the Sahel as a Function of Weather Type, Using Neural Network Methodology, J. Geophys. Res.: Atmospheres, 118, 13, 265–13, 281, https://doi.org/10.1002/2013JD019465, 2013.